On different parameterisation methods to analyse spacecraft attitude manoeuvres in the presence of attitude constraints

G. Radice and M. Casasco
Department of Aerospace Engineering
University of Glasgow
Scotland, UK

ABSTRACT

This paper analyses and compares two different attitude representations, using quaternions and modified Rodrigues parameters, in the context of the potential function method applied to autonomously control constrained attitude slew manoeuvres. This method hinges on the definition of novel Lyapunov potential functions in terms of the attitude parameters representing the current attitude, the goal attitude and any pointing constraints, which may be present. It proves to be successful in forcing the satellite to achieve the desired attitude while at the same time avoiding the pointing constraints. A linearised version of the modified Rodrigues parameterisation is also introduced and analysed. Finally advantages and drawbacks of all attitude representations are discussed.

NOMENCLATURE

A	shaping parameter
B	shaping parameter
k_D	proportional-derivative controller parameter
k_{ii}	weighting coefficients
k_p	proportional-derivative controller parameter
q	quaternion
q_c	current attitude quaternion
q_g	commanded attitude quaternion
q_{ob}	obstacle quaternions
V	lyapunov function
V_a	attractive component of Lyapunov function
V_{rep}	repulsive component of Lyapunov function
x	state vector
λ	shaping parameter
ν	shaping parameter
σ	modified Rodrigues parameter
σ_c	current attitude modified Rodrigues parameter
σ_g	commanded attitude modified Rodrigues parameter
σ_{ob}	obstacle modified Rodrigues parameter
σ_s	shadow set
$\bar{\sigma}$	constant attitude vector
ω	angular velocity vector
ω_{cs}	required angular velocity
ω_{av}	obstacle avoidance angular velocity

Paper No. 2991. Manuscript received 1 July 2005, revised 15 September 2005, 2nd revision 31 March 2006, accepted 19 March 2007.

https://doi.org/10.1017/S0001924000004589 Published online by Cambridge University Press

1.0 INTRODUCTION

Performing constrained attitude slew manoeuvres is currently a common problem for many spacecraft missions. The constraints often arise from payload safety reasons: usually they consist in either not directing delicate instrumentation (typically infrared and optical instruments) towards bright sky regions or avoiding blinding of attitude sensors. For example a cryogenically cooled infrared telescope has to be slewed between astronomical targets without directing the payload towards the Sun, Moon, or any other infrared bright region of the sky. Moreover, three-axis stabilised satellites must perform manoeuvres to safe pointing modes in case of failure without blinding attitude sensors. The problem of performing constrained attitude slews has traditionally been addressed by exploiting conventional approaches[1-3]: open-loop approaches enable the calculation of high-precision solutions that minimise a user-prescribed cost functional, such as fuel consumption or manoeuvre time. However, these approaches usually involve iterative procedures and are hence, in most cases, computationally expensive and not completely reliable. Closed loop or feedback approaches perform only non-iterative procedures and calculate the current control action based on the current state. Feedback approaches typically perform at best near optimality, and for nonlinear controllers or nonlinear dynamical systems, it is not easy to guarantee that the controller is always able to drive the states to the goal values. Moreover, it is usually difficult to enforce state constraints. More recently, new control techniques, relying on artificial intelligence or expert systems[4], introduced with the aim of allowing autonomous real time on-board control, proved to require significant on-board computational capabilities. Other approaches using neural networks[5]), although successful are difficult to explicitly validate. Additionally, the complexity of specific spacecraft control problems is largely due to the nonlinear dynamics and uncertainties of the problem under analysis. To better account for these features, many nonlinear approaches have been applied to spacecraft dynamics: typical nonlinear approaches include sliding mode control[6], input-output feedback linearisation[7] and output regulation theory[8]. The potential function method represents a novel non-linear approach to the problem of attitude control. Potential function methods have been used for autonomous guidance and control systems applied to terminal descent to a planetary surface[9], to constrained proximity manoeuvring for space station rendezvous[10], to formation flying[11] and to attitude control[12]. This paper presents the stability and control analysis of large angle feedback slew manoeuvres with pointing constraints. Different representations of the spacecraft attitude are considered: quaternions, modified Rodrigues parameters and a linearised form of the modified Rodrigues parameters are the selected attitude parameterisations.

2.0 THE POTENTIAL FUNCTION METHOD

The potential function method is an extension of Lyapunov's second method. This method has found a number of applications in the space field for the generation of closed-loop control functions with the advantage of allowing the implementation of non-linear controls, since the method does not hinge on linearisation. Given a set of differential equations $\dot{y} = f(x)$, which describe the time evolution of a dynamic system, and defining the desired final state, the convergence to this state and the global stability of the system can be guaranteed by building a Lyapunov potential function that has a global minimum in the final state. In fact, a function $V = V(x)$ is a Lyapunov function for the system if the following conditions are met:

$$V(\bar{x}) = 0 \qquad \ldots (1(a))$$

$$V(x) > 0 \quad for\ x \neq \bar{x} \qquad \ldots (1(b))$$

$$V(x) \to \infty \quad for\ \|x\| \to \infty \qquad \ldots (1(c))$$

$$\dot{V}(x) \leq 0 \quad for\ x \neq \bar{x} \qquad \ldots (1(d))$$

for the goal state $\bar{x}$.

Lyapunov's theorem guarantees that a system that admits such a Lyapunov function is globally stable. Moreover, once the final target state has been defined, it is possible to consider stability and control as equivalent. We will consider two possible kinematics equations: one based on quaternions, and one based on modified Rodrigues parameters. Since the kinematics equation of all attitude parameterisations provide a relationship between the attitude parameters and the angular velocities in the form of a differential equation, the kinematics model is cascaded to the dynamics model. In fact, the angular velocities are both the output of the dynamics model and the input of the kinematics model. This particular feature of the system in the rigid body control problem allows two different regulators for the two models to be employed: the control system over the kinematics model, given the goal values of the kinematics parameters, determines the required angular velocities, while the control system over the dynamics model calculates the torque needed to track these required angular velocities. In this work, we will consider a potential function control for the kinematics subsystem and a proportional-derivative regulator for the dynamics model.

3.0 QUATERNION BASED PARAMETERISATION

As previously explained, the convergence towards the goal attitude is achieved through the attractive component of the potential function, the stability (control) properties of which can be validated with the Lyapunov theorem. The first step in the control system synthesis is the choice of the state variables to be used to build the potential function. In this section we will consider the quaternions as the state variables. They are a once-redundant set of rotation parameters, bounded to satisfy the constraint of unity norm. This means that all possible trajectories generate arcs on the surface of a four-dimensional unit sphere, thus bounding the quaternions to values between 1 and –1. They are not unique, since the same physical location can be described by two different sets of quaternions, which differ by a sign. The two sets represent respectively a clockwise and a counter clockwise rotation about the same principal rotation axis of angles differing by 360 degrees, thus describing the same orientation[13].

The chosen state variables are, more precisely, the error quaternion, which are the set of quaternion elements that express the rotation required to reach the target attitude from the current attitude. In fact the commanded attitude quaternion $q_g = (q_{1g}, q_{2g}, q_{3g}, q_{4g})$ and the current attitude quaternion $q_c = (q_{1c}, q_{2c}, q_{3c}, q_{4c})$ are related to the error quaternion $q = (q_1, q_2, q_3, q_4)$ as follows[14]:

$$\begin{bmatrix} q_1 \\ q_2 \\ q_3 \\ q_4 \end{bmatrix} = \begin{bmatrix} q_{4g} & q_{3g} & -q_{2g} & -q_{1g} \\ -q_{3g} & q_{4g} & q_{1g} & -q_{2g} \\ q_{2g} & -q_{1g} & q_{4g} & -q_{3g} \\ q_{1g} & q_{2g} & q_{3g} & q_{4g} \end{bmatrix} \cdot \begin{bmatrix} q_{1c} \\ q_{2c} \\ q_{3c} \\ q_{4c} \end{bmatrix} \qquad \ldots (2)$$

Since changing the signs of all the quaternion elements simultaneously does not change the parameterised attitude, the target values for the state variables (error quaternion) are both $\boldsymbol{q} = [0\ 0\ 0\ 1]^T$ and $\boldsymbol{q} = [0\ 0\ 0\ -1]^T$. To account for this, the potential function must be built in order to have global minima in both target states. Thus, the attractive component of the potential function is expressed as follows:

$$V_a = q_1^2 + q_2^2 + q_3^2 + \left(|q_4| - 1\right)^2 \qquad \ldots (3)$$

https://doi.org/10.1017/S0001924000004589 Published online by Cambridge University Press

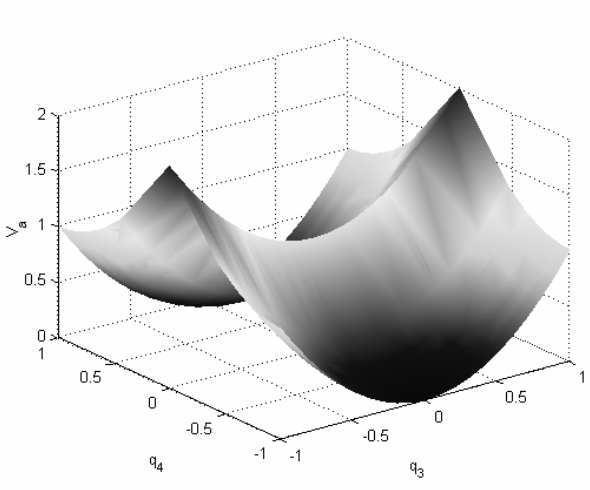

Figure 1. Visualisation of the potential function for a rotation around a principal inertia axis, described with quaternions.

Equation (3) is a quadratic form of all four quaternion elements, with two as the maximum value of the potential and global minima in the target values of the attitude. The following figure shows the shape of the potential function as a function of q_3 and q_4, with q_1 and q_2 are set to zero: the presence of two global minima, which describe the same final state is easily noticeable.

Within the context of potential function control, the pointing constraint requirements are easily introducible and controllable. The basic concept that leads to prevent pointing towards the constraint is placing a large potential around the constrained direction. Due to the nature of the control methodology, the manoeuvre will however be non optimal, regardless of the size of the avoidance cone. The technical literature presents different forms of the component of the potential function that can be used to implement this feature. In the present work, the repulsive capability is achieved through the following exponential function:

$$V_{rep} = A \cdot e^{-B\left[q_{ob1}{}^2 + q_{ob2}{}^2 + q_{ob3}{}^2 + \left(|q_{ob4}| - 1\right)^2 \right]} \quad \ldots (4)$$

where $q_{ob} = [q_{ob1}\ q_{ob2}\ q_{ob}3\ q_{ob4}]^T$ is the quaternion representing the constrained direction – a direction that has to be avoided for payload or instrument safety – in an inertial frame of reference, and A and B are shaping parameters. The choice of exponential functions to implement the repulsive component of the potential function represents a compromise between accuracy and computational complexity because they are simple and suitable to describe pointing constraints in terms of separation from a direction. With the use of different values for the parameters A and B, it is possible to define the increase or decrease and alter the shape of the constrained area. The reliability of the method hinges on Lyapunov's theorem, so an attitude requirement close to a constraint region can be achieved. This however will most likely require a careful selection of the shaping parameters.

The control system is endowed with the pointing avoidance capability as well as the convergence capability by introducing a total potential function, built as the sum of the attractive and repulsive potentials we obtain the following expression of the potential function:

$$V = q_1^2 + q_2^2 + q_3^2 + \left(|q_4| - 1\right)^2 + A \cdot e^{-B\left[q_{ob1}{}^2 + q_{ob2}{}^2 + q_{ob3}{}^2 + \left(|q_{ob4}| - 1\right)^2\right]} \quad \ldots (5)$$

Because of the form that the composition of rotations assumes in terms of quaternion elements, Equation (5) is function of five variables, three components of q, representing the rotation needed to reach the goal attitude and two components of qob, representing the direction of the constrained direction. A straightforward remark is that the introduction of more pointing constraints requires the introduction of two new variables for each new constraint, as the angular orientation along the axis of the instrument that has to avoid the constrained direction is free. The final commanded angular velocity is then calculated from the difference between the current angular velocity and the required angular velocity:

$$\Delta\omega = \omega - \omega_c \quad \ldots (6)$$

where ω is the angular velocity vector in body-fixed frame, and ω_c is the angular velocity vector that must be supplied by the actuators to slew the spacecraft towards the desired attitude while at the same time avoiding any pointing constraints. The expression for ω_c is:

$$\omega_c = 2\Xi\dot{q} = -2\Xi\nu\left(1 - e^{-\lambda V}\right)\frac{\nabla V}{\|\nabla V\|} \quad \ldots (7)$$

where λ and ν are shaping parameters and Ξ is the matrix of quaternion kinematics.

4.0 MODIFIED RODRIGUES PARAMETERISATION

To address the problem of singular orientations while using a minimal set of three rigid body attitude coordinates, the modified Rodrigues parameters have been recently proposed. They are derived from the quaternions through stereographic projection; the transformation is the following:

$$\sigma_i = \frac{q_i}{1 + q_4} \qquad i = 1, 2, 3 \quad \ldots (8)$$

where $\sigma = [\sigma_1\ \sigma_2\ \sigma_3]^T$ is the vector of the modified Rodrigues parameters. Like the quaternions, the modified Rodrigues parameters are not unique, and reversing the signs of the q_i in Equation (8) generates a second set of σ_i. This alternative set is called 'shadow set' and the transformation from the original set to the shadow set is:

$$\sigma_s = \frac{-\sigma}{\sigma^T\sigma} \quad \ldots (9)$$

where σ_s is the shadow set. Both σ and σ_s describe the same physical orientation, similar and related to the case of the two possible sets of quaternions and principal rotation vectors. The modified Rodrigues shadow parameters have the opposite singular behaviour to the original ones. The original parameters are linear near a zero rotation and are singular at a ±360° rotation. The shadow parameters are linear near the ±360° rotation and singular at the zero rotation. Since both sets satisfy the same equation of motion, only differing in initial conditions, the advantage of using modified Rodrigues parameters is that if a singularity is encountered with the original set, by switching to the shadow set the singularity can be avoided and vice versa. The only effect of switching parameters is the discontinuity that occurs at the switching point. The choice in distinguishing between the two sets is purely arbitrary so the choice of $\sigma^T\sigma = 1$ implies that the magnitude of the orientation vector is bounded between 0 and 1, which means that the principal rotation angle is restricted to ±180°. Once again, the choice of the state variables to build the potential function is subject to the consideration that the rotation required to reach the target attitude σ_g from the current attitude σ_c is expressed, in terms of modified Rodrigues parameters, as:

$$\sigma = \frac{\left(1 - \sigma_g^T\sigma_g\right)\sigma_c - \left(1 - \sigma_c^T\sigma_c\right)\sigma_g + 2\sigma_c \times \sigma_g}{1 + \left(\sigma_g^T\sigma_g\right)\left(\sigma_c^T\sigma_c\right) + 2\sigma_c \bullet \sigma_g} \quad \ldots (10)$$

The vector $\sigma = [\sigma_1\ \sigma_2\ \sigma_3]^T$ now represents the attitude error modified Rodrigues parameters and is used to build the potential function. The attractive component of the potential function can now

https://doi.org/10.1017/S0001924000004589 Published online by Cambridge University Press

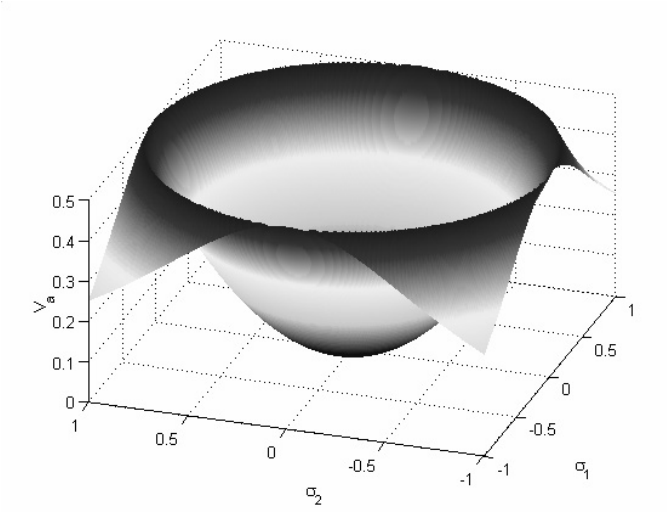

Figure 2. Visualisation of the potential function for the variation of two modified Rodrigues parameters. Notice the maximum values in correspondence of the circumference with unit radius (switching line in the considered example).

be written as a quadratic function of the three modified Rodrigues parameters, as follows:

$$V_a = \frac{1}{2}\sigma_1^2 + \frac{1}{2}\sigma_2^2 + \frac{1}{2}\sigma_3^2 \quad \ldots (11)$$

Equation (11) has a maximum at 0·5 in correspondence of the switching condition between the original and the shadow sets. The following figure shows the shape of the potential function for the variation of two modified Rodrigues parameters.

The change in the sign of the derivative of the potential function in correspondence of the switching condition is due to the use of the shadow set in Equation (11) to calculate the value of V, while Fig. 2 reports only the original values of σ_1 and σ_2 along the axes. The behaviour of the potential function outside the switching condition also suggests that four more global minima are present for the different combinations of ±360° rotations described by the parameters σ_1 and σ_2. As previously done for the case of quaternions, the repulsive capability is achieved through the following exponential function:

$$V_{rep} = A \cdot e^{-B\left[\sigma_{ob1}{}^2 + \sigma_{ob2}{}^2 + \sigma_{ob3}{}^2\right]} \quad \ldots (12)$$

where $\sigma_{ob} = [\sigma_{ob1}\ \sigma_{ob2}\ \sigma_{ob3}]^T$ are the modified Rodrigues parameters representing the constrained direction, while A and B are shaping parameters. In order to endow the control system with the pointing avoidance capability as well as the convergence capability, a total potential function, built as the sum of the attractive and repulsive potentials, is introduced:

$$V = \frac{1}{2}\sigma_1^2 + \frac{1}{2}\sigma_2^2 + \frac{1}{2}\sigma_3^2 + A \cdot e^{-B\left[\sigma_{ob1}{}^2 + \sigma_{ob2}{}^2 + \sigma_{ob3}{}^2\right]} \quad \ldots (13)$$

The final commanded angular velocity is then calculated from the difference between the current angular velocity and the required angular velocity:

$$\Delta\omega = \omega - \omega_c \quad \ldots (14)$$

where ω is the angular velocity vector in body-fixed frame, and ω_c, introduced in Equation (7), is the angular velocity vector that must be supplied by the actuators to slew the spacecraft towards the desired attitude while at the same time avoiding any pointing constraints. A proportional-derivative controller finally tracks the required difference in angular velocities.

5.0 LINEARISED MODIFIED RODRIGUES PARAMETERISATION

As previously highlighted, both the use of the quaternions and of the modified Rodrigues parameters implies the initiation of an increasingly large number of parameters to be integrated and controlled as multiple pointing constraints are introduced. This is basically due to the nonlinear form of Equations (2) and (10), which do not allow expressing the attitude error parameters in a more simple form. It appears to be interesting, then, to investigate what happens if the expression that yields the relative rotation between two sets of kinematics parameters is linearised. Because of the strict constraint that bounds the values of the quaternions, a linearisation of Equation (2) that maintains the unity norm of the quaternions is not possible. On the other hand, the modified Rodrigues parameters can easily be linearised. By observing the form of Equation (10), it is easy to notice that, for small angles, it becomes:

$$\sigma \cong \sigma_c - \sigma_g \quad \ldots (15)$$

Equation (15) is a linear relation that allows an easy, though approximate, calculation of the attitude error. It reflects the previously highlighted features of linearity of the modified Rodrigues parameters: very good linearity for near zero rotations (that is for small angles) and near the ±360° rotation (thanks to the introduction of the shadow set), and approximated results for rotations of intermediate magnitude, that is near the switching surface. The aim of this linearisation is two fold: to show that the controller is stable even though large angle slews are performed and to evaluate the performance of the controller when an approximation of the angular error is used. By exploiting Equation (15), it is now possible to write the potential function for the control with modified Rodrigues parameterisation in the following form:

$$V_a = \frac{1}{2}\left(\sigma_1 - \bar{\sigma}_1\right)^2 + \frac{1}{2}\left(\sigma_2 - \bar{\sigma}_2\right)^2 + \frac{1}{2}\left(\sigma_3 - \bar{\sigma}_3\right)^2 \quad \ldots (16)$$

where $\sigma = [\sigma_1 \sigma_2 \sigma_3]^T$ is the vector of the current attitude parameters, and $\bar{\sigma} = \left[\bar{\sigma}_1 \quad \bar{\sigma}_2 \quad \bar{\sigma}_3\right]^T$ is the constant vector of the goal attitude in terms of modified Rodrigues parameters. Switching to the shadow set is still possible, thus the shape of the potential function is completely similar to that represented in Fig. 2. The repulsive capability is achieved through the following exponential function:

$$V_{rep} = A \cdot e^{-B\left[\left(\sigma_1 - \sigma_{ob1}\right)^2 + \left(\sigma_2 - \sigma_{ob2}\right)^2 + \left(\sigma_3 - \sigma_{ob3}\right)^2\right]} \quad \ldots (17)$$

where $\sigma_{ob} = [\sigma_{ob1}\ \sigma_{ob2}\ \sigma_{ob3}]^T$ arethe modified Rodrigues parameters representing direction of the constraint, but now, because of the use of Equation (15), they are constants. The global potential function therefore is:

$$V = \frac{1}{2}\sigma_1^2 + \frac{1}{2}\sigma_2^2 + \frac{1}{2}\sigma_3^2 + \quad A \cdot e^{-B\left[\left(\sigma_1 - \sigma_{ob1}\right)^2 + \left(\sigma_2 - \sigma_{ob2}\right)^2 + \left(\sigma_3 - \sigma_{ob3}\right)^2\right]} \quad \ldots (18)$$

The potential function in Equation (18) does not show the same behaviour of the potential functions in Equations (5) and (13): in fact it is now a function of three variables, since both the rotation that would lead the spacecraft to target attitude and the rotation that would force the body-axes to point towards the constrained direction are expressed as the difference of the current modified Rodrigues parameters and the constant components of vectors $\bar{\sigma}$ and σ_{ob}. The only variables are now the three components of σ. It is a remarkable feature of the linearised parameterisation via modified Rodrigues parameters that the introduction of more constrained attitudes does

https://doi.org/10.1017/S0001924000004589 Published online by Cambridge University Press

not require the introduction of new variables. The final commanded angular velocities are finally calculated from the difference between the current angular velocities and the required angular velocities:

$$\Delta\omega = \omega - \omega_c \quad \ldots (19)$$

where ω is the spacecraft's angular velocity and ω_c, introduced in Equation (7), is the required angular velocity that the actuators must produce in order to have the satellite pointing towards the required direction while still avoiding the constrained attitudes. The required difference in angular velocities is once again tracked by a proportional-derivative controller.

6.0 NUMERICAL SIMULATIONS

All the described control systems have been implemented and simulated in the Matlab/Simulink environment. The aim of the numerical analysis is to provide results for a sample of meaningful manoeuvres to be used as the basis for the evaluation of the control performances. The spacecraft is considered to be a three-axis stabilised satellite controlled through a continuous torque control, capable of providing torques of up to 30Nm around each principal axis. Actuator dynamics and sensor accuracy and filtering are neither modelled nor taken into account since they are not relevant for the purpose of evaluating and comparing the performances of the three different potential function controllers. The simulation chosen to illustrate the behaviour of the controllers is also useful to highlight some features of the selected potential functions and to illustrate the corrections required in specific cases to escape possible failures in reaching the required attitude. In fact, since the repulsive component of all the previously illustrated controllers describes symmetric constraints, in a limited number of cases, the control system might not be able to select between two equivalent (in terms of the potential function) paths, thus failing to overcome the constraint and reach the goal attitude.

One representative case of this behaviour consists in having initial and goal attitudes placed such that a rotation of ±180° around one of the principal axes is required, with two equally spaced constraints between the initial and the goal attitude (that is placed at ±90° around the principal axis). If the constraints are perfectly symmetric, the two possible commanded rotations of ±180° and −180° required to reach the goal are completely equivalent in terms of potential: this means that the system is in the situation represented, for example, in Fig. 1 by the unstable equilibrium points placed along the $q_4 = 0$ coordinate. Given that the actual system is subject to perturbations, and that the equilibrium is unstable, the symmetry of the system is somewhat broken and all the previously illustrated controllers are able to discriminate between the two possible rotations. Once the commanded rotation forces the spacecraft to rotate around the principal axes, one of the pointing constraints is approached: the closer the constraint, the larger the repulsive component of the potential. This process continues until the repulsive component of the potential is large enough to overcome the value of the attractive component, thus commanding the action of the controller to prevent the infringement of the constraint. However, because of the symmetric nature of the constraint, the control action does not force the rotation to continue out of the plane perpendicular to the principal axis in order to overcome the constraint, but simply implies that the rotation stops at a saddle point near the constrained attitude. The previous remarks about equilibrium instability and perturbed motion imply that the saddle is eventually escaped but the process is so slow and expensive in terms of control effort that an alternative solution is needed. The selected approach fulfils two goals, namely to force the potential to be asymmetric and to increase the component of the torque required to have an out-of-plane rotation.

The first goal is implemented by artificially displacing the constraint: the orientation of the constrained attitude is modified by adding a small error term to the kinematics parameters (and then re-normalising in the case of the quaternions). Consequence of this is that the analytical constraint does no longer match the physical constraint from which it arose: thus an encroachment of the physical constrained area is likely. To avoid this problem, however, it is sufficient to increase the size of the analytical constrained area, by modifying the values of the parameters A and B in the equation of the repulsive component of the potential function.

The second goal is achieved by modifying the repulsive component of the potential function in all the employed forms, that is Equations (4), (12) and (17). This is accomplished by expressing these equations respectively as:

$$V_{rep} = A \cdot e^{-B\left[k_{11}\cdot q_{ob1}^2 + k_{22}\cdot q_{ob2}^2 + k_{33}\cdot q_{ob3}^2 + k_{44}\cdot\left(|q_{ob4}| - 1\right)^2\right]} \quad \ldots (20)$$

$$V_{rep} = A \cdot e^{-B\left[k_{11}\cdot \sigma_{ob1}^2 + k_{22}\cdot \sigma_{ob2}^2 + k_{33}\cdot \sigma_{ob3}^2\right]} \quad \ldots (21)$$

$$V_{rep} = A \cdot e^{-B\left[k_{11}\cdot(\sigma_1 - \sigma_{ob1})^2 + k_{22}\cdot(\sigma_2 - \sigma_{ob2})^2 + k_{33}\cdot(\sigma_3 - \sigma_{ob3})^2\right]} \quad \ldots (22)$$

The introduction of weight coefficients k_{ii} is intended to increase the repulsive force in the out-of-plane direction: this is actually accomplished by reducing the coefficient relative to the axis perpendicular to the plane of rotation. For example, if the rotation takes place in the x-y plane, it is necessary to decrease the value of the coefficient relative to the z axis, that is k_{33}. It is remarkable that in Equation (20) a fourth weight coefficient has been added: it is relative to the scalar component of the quaternions and its physical interpretation is not immediate. However, its introduction has proved useful in forcing the rotation out-of the plane, by decreasing its value together with that of another coefficient. The performed simulations showed that the manoeuvres are sensitive to the values of the weight coefficients: moreover the dependence of the problem from initial and goal conditions and the difficulty of associating a physical meaning to some coefficients testify how difficult is to implement a strategy for choosing the weight parameters. No explicit strategy has been implemented within this work, but it seems realistic that the laws that will be used to calculate the values of the kii coefficients should take into account the initial and goal conditions and the constrained orientations, thus promoting the control to be self-tuning or adaptive, with the relative advantages and drawbacks.

The values of the parameters, for all the different controllers, are: $\nu = 0{\cdot}1$rad/s, $\lambda = 50$ – see Equation (7) – $A = 1$ and $B = 100$. The obstacles are identified by the following parameters: $q_{ob1} = (0, 0, 1/\sqrt{2}, 1/\sqrt{2})$, $q_{ob2} = (0, 0, -1/\sqrt{2}, 1/\sqrt{2})$, $\sigma_{ob1} = (0, 0, 1/(1+\sqrt{2}))$, $\sigma_{ob2} = (0, 0, -1/(1+\sqrt{2}))$. Moreover, the displacement of the constraints has been implemented by adding an artificial error of $0{\cdot}005$ to q_{ob1} and q_{ob2} (and re-normalising) for the quaternions-based parameterisation, to σ_{ob1} and σ_{ob2} for the modified Rodrigues parameterisation and to the differences $(\sigma_1 - \sigma_{ob1})$ and $(\sigma_2 - \sigma_{ob2})$ for the linearised modified Rodrigues parameterisation. The out-of-the-plane torque has been increased by imposing a value of $0{\cdot}2$ for the k_{33} coefficients of both the modified Rodrigues parameterisations, and a value of $0{\cdot}2$ for both the k_{33} and k_{44} coefficients of the quaternions-based parameterisation. Since the unbalanced torque generation is not useful when approaching the goal position, the previously listed coefficients are set to 1 respectively for $|\sigma_3| < 0{\cdot}9$ (modified Rodrigues parameterisation) and $|q_4| < 0{\cdot}9$ (quaternions-based parameterisation). The remaining kii coefficients have all been set to 1. The coefficients of the proportional-derivative regulators are the same for each component of the angular velocity in all the implemented control systems. Considering the usual form of the proportional-derivative controller, here reported as:

$$u = k_P \cdot \omega + k_D \cdot \dot{\omega} \quad \ldots (23)$$

https://doi.org/10.1017/S0001924000004589 Published online by Cambridge University Press

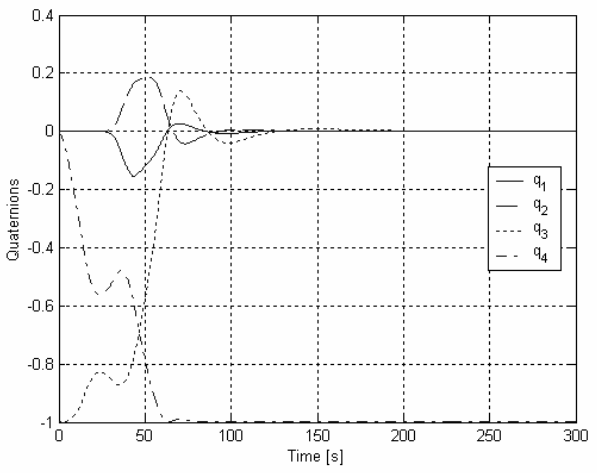

Figure 3. Time history of the quaternions.

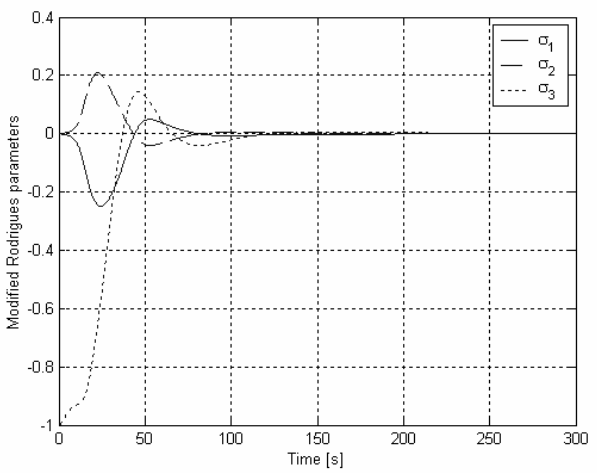

Figure 4. Time history of the modified Rodrigues parameters.

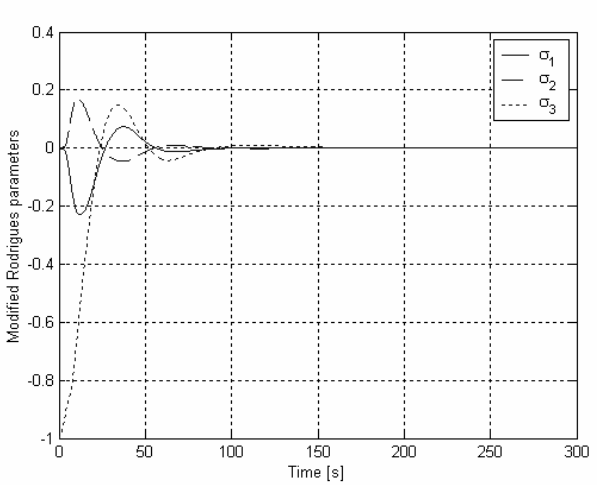

Figure 5. Time history of the linearised modified Rodrigues.

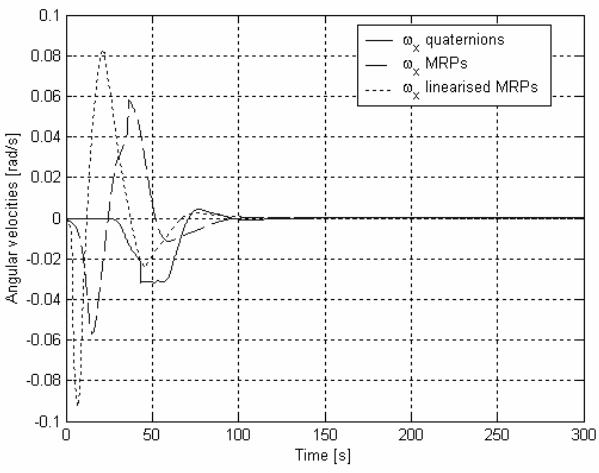

Figure 6. Time history of angular velocities around the – axis.

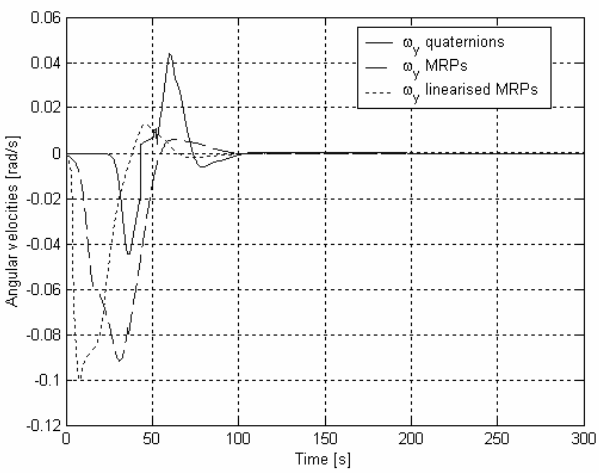

Figure 7. Time history of angular velocities around the *y*-axis.

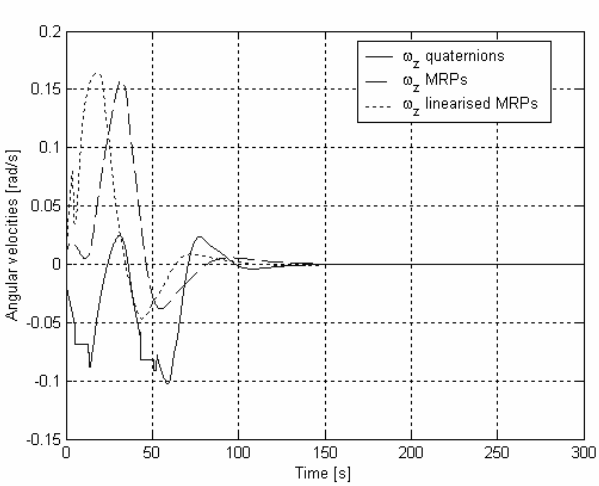

Figure 8. Time history of angular velocities around the *z*-axis.

https://doi.org/10.1017/S0001924000004589 Published online by Cambridge University Press

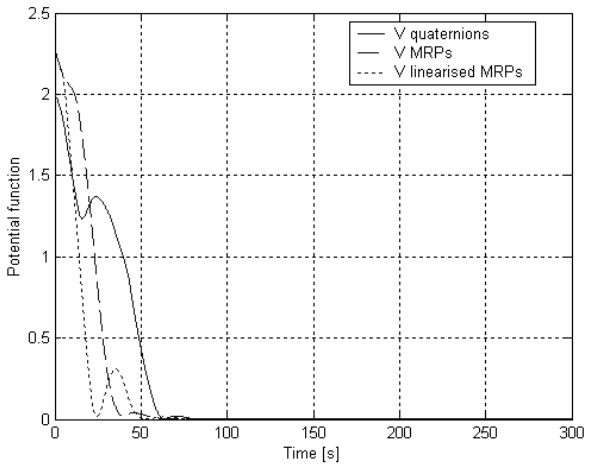

Figure 9. Evolution of the potential functions.

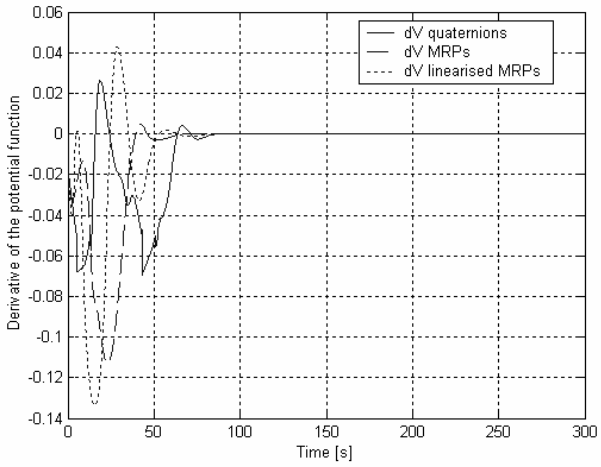

Figure 10. Evolution of the derivatives of the potential function.

where u and ω are referred to a generic component, and the chosen values for the coefficients are: $k_p = 15$ and $k_D = 5$. The integration technique chosen to solve the system composed by the dynamics equations and the kinematics equations is based on the fifth-order Dormand-Price formula. The following figures compare the time history of the kinematics parameters for the three control systems under analysis. In Fig. 3, it is shown how the vector part of the quaternions, that is q_1, q_2, and q_3, converges to zero, thus proving the achievement of the goal attitude, while the scalar part, q_4, converges to –1, thus preserving the constraint on the norm of the quaternions. It is interesting to note that q_1 and q_2 are initially displaced from their initial state in order to overcome the constrained attitude, and later converge again to the initial state, also correspondent to the final state. In Fig. 4, the convergence of the error modified Rodrigues parameters is represented: it is again noticeable that σ_1 and σ_2 are displaced from their initial state and converge to zero after the constraint is overcome. The same features are present in Fig. 5, where the convergence and capability of complying with the pointing constraint of the linearised modified Rodrigues parameters are shown.

In the following figures the angular velocities obtained with the three control systems under analysis are compared. Figure 6 compares the angular velocities of the spacecraft around the x-axis. The angular velocities are forced to move out of the plane, thus allowing the constraint to be overcome. The controller based on linearised modified Rodrigues parameters commands the maximum values of angular velocity during the manoeuvre. The velocity profiles with modified Rodrigues parameters and with linearised modified Rodrigues parameters are similar: the response of the linearised modified parameters is slightly faster and the values of the velocity slightly larger. The profile with the quaternions is more regular and with smaller values of velocity. Figure 7 represents the angular velocities of the spacecraft around the y-axis. The maximum velocity is once again achieved with the linearised modified Rodrigues parameters, while the response of the controller with the modified Rodrigues parameters is slower and implies a smaller velocity, whilst the velocity profile achieved with the quaternions is nearly symmetric. Figure 8 shows the angular velocities of the spacecraft around the z-axis: the rotation around the z axis is counter-clockwise both with the modified Rodrigues parameterisation and with the linearised modified Rodrigues parameterisation, while the quaternions-based controller commands a clockwise rotation. The direction of rotation around the z-axis is the consequence of the different implementation of the displacement of the symmetric constrained attitudes.

The velocity profile achieved with the quaternions-based controller is subject to a change in the sign of the angular velocity in the 24-36 seconds period, thus testifying that the constraint is overcome in two steps: at first, the spacecraft bounces back against the constraint, but in the meantime the rotations around the x and y axes allow the constrained attitude to be overcome after nearly 50 seconds. In the following figures (Figs 9-10), the convergence of the potential function to zero is shown for all the control systems under analysis alongside with the evolution of the derivatives of the potential function.

The values of the potential functions, expressed by Equations (13) and (18), and of their derivatives, relative to the nonlinear and linearised modified Rodrigues parameterisations, have been multiplied by four in order to be represented in the same scale as the potential function and derivative obtained using the quaternion representation. As far as the potential function relative to the quaternion-based control is concerned, it is noticeable from Fig. 9, and confirmed by Fig. 10, that in the span of 15-25 seconds of simulation the potential function increases: this behaviour is forced by the control system in order to escape the saddle in the potential function close to the attitude constraint. A second increase in the value of the potential function takes place after 60 seconds of simulation and it is due to the fact that the spacecraft either reaches the goal attitude or moves close to it, but when it starts to move further, the momentum is too large to be immediately compensated with the available torque. The same behaviour is shown by the other control systems: the increase in the value of the potential function relative to the modified Rodrigues parameterisation takes place after 40 seconds, while that of the potential function relative to the linearised modified Rodrigues parameters takes place after 25 seconds and is much larger than the others. The following figures show the time history of the control torques.

The main feature of these figures is that the actuators perform continuous torques of small magnitude (up to 2Nm), alternated by much larger impulses. The reason of this behaviour is that the proportional-derivative controller continuously tracks the commanded angular velocity, thus performing the continuous corrective torques, while the commanded angular velocity is controlled by the potential function control system in a discontinuous way: that is the commanded angular velocity is different from zero only when the derivative of the potential function is larger than a fixed threshold. In order to guarantee convergence, the value of this threshold has to be negative: in this work a fixed value of the threshold equal to – 0·05 has been employed. In Fig. 12, we can notice that the control torques exerted by the control system based on modified Rodrigues parameters present a fewer number of impulses, with respect to Fig. 11, thus implying a fewer number of

https://doi.org/10.1017/S0001924000004589 Published online by Cambridge University Press

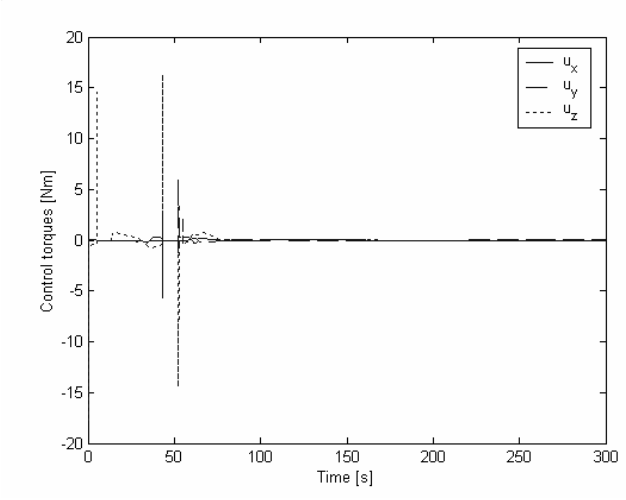

Figure 11. Applied control torques during the manoeuvre accomplished with the quaternions-based control system.

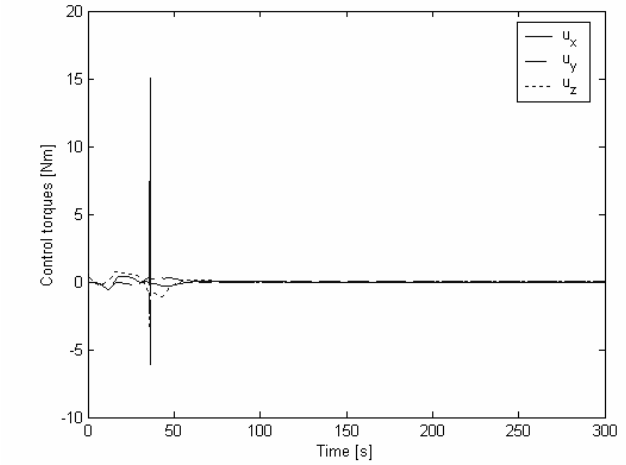

Figure 12: Applied control torques duzring the manoeuvre accomplished with the control system based on modified Rodrigues parameters.

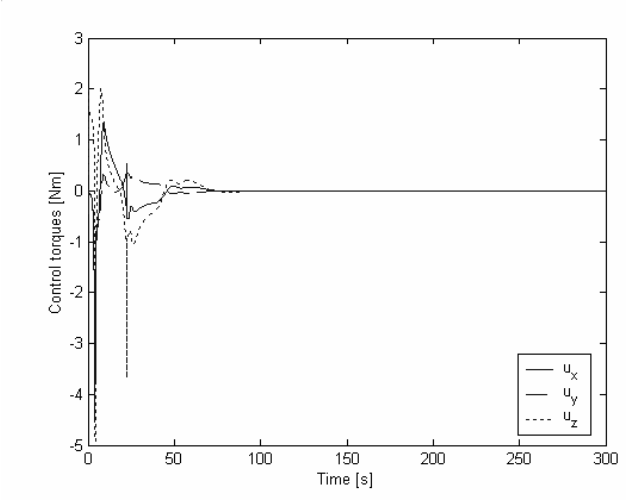

Figure 13. Applied control torques during the manoeuvre accomplished with the control system based on linearised modified Rodrigues parameters.

relevant attitude corrections. Moreover, the magnitude of the impulses is lower, with the relevant consequence of less control effort. Figure 13 shows the control torques for the control system based on the linearised modified Rodrigues parameters: the magnitude of the impulses is smaller than in the previous cases, but the total control expense is larger than with the controller based on modified Rodrigues parameters, even if smaller than that with the quaternions-based controller.

7.0 CONCLUSIONS

In this paper, the problem of autonomous slew manoeuvring has been addressed within the context of the potential function method. Three controllers based on different kinematics parameterisations have been analysed and compared. Alongside with well-known quaternions and modified Rodrigues parameterisations, a new linearised form of the modified Rodrigues parameters has been introduced in order to decrease the computational complexity of the problem. All the control systems, respectively based on quaternions, modified Rodrigues parameters, and linearised modified Rodrigues parameters, have proved to be able of reaching the goal attitude, in accordance with the Lyapunov theorem, whilst complying with the pointing constraints. Future extension of this work will centre in three directions. To add one or more forced directions; that is a direction that the spacecraft has to maintain: for example constantly pointing the solar panels towards the Sun. To investigate the possibility of having attitude requirements that are very close to constrained regions through an appropriate selection of the shaping parameters in the Lyapunov function. Finally, we will consider an optimisation, in terms of fuel consumption and time, of the manoeuvre.

REFERENCES

1. VADALI, S.R. and JUNKINS, J.L. Spacecraft large angle rotational maneuvers with optimal momentum transfer, *J Astronautical Sciences*, **XXXI**, (2), 1983, pp 217-235.
2. WIE, B. and BARBA, P.M. Quaternion feedback for spacecraft large angle maneuvers, *J Guidance, Control and Dynamics*, 1985, **8**, (3), pp 360-365.
3. STEYN, W. and HASIDA, H. An attitude control system for a low-cost earth observation satellite with orbit maintenance capability, 13th AIAA Conference on Small Satellites, USA, 1999.
4. OLSZWESKI, O.W. Automated terminal guidance for a shuttle rendezvous to space station freedom, proceedings of the AIAA guidance, Navigation and Control Conference, AIAA, 1990 Washington DC, USA, pp 337-387.
5. CARRARA, V. and RIOS NETO, A. A Neural network satellite attitude controller with error based reference trajectory, XIV International Symposium on Space Flight Dynamics, Brazil, 1999.
6. SINGH, S.N. and IYER, A. Nonlinear Decoupling Sliding Mode Control and Attitude Control of Spacecraft, IEEE Transactions on Aerospace and Electronic Systems, 1989, **25**, (5), pp 621-633.
7. SLOTINE, J.J.E. and LI, W. *Applied Nonlinear Control*, Prentice Hall, 1991.
8. ISIDORI, A. and BYRNES, C.I. Output regulation of nonlinear systems, IEEE transactions on automatic control, 1990, **35**, (2), pp 131-140.
9. MCINNES, C.R. Path Constrained manoeuvring using artificial potential functions, *European Space Agency J*, 1993, **17**, (2), pp 159-169.
10. ROGERS, A.B. and MCINNES, C.R. Safety constrained free-flyer path-planning at the international space station, *J Guidance, Control and Dynamics*, 2000, **23**, (6), pp 971-980.
11. RADICE, G. Deployment considerations for spacecraft formation at sun-earth L2 Point, 4th Workshop on Satellite Constellations and Formation Flying, Sao Jose dos Campos, Brazil, 2005.
12. RADICE, G. and MCINNES, C.R. Multiple target selection and obstacle avoidance using potential function guidance method, AAS/AIAA Astrodynamics Specialists Conference, 2001, Quebec City, Canada.
13. CHOBOTOV, V.A. Orbital mechanics, AIAA Education Series, 2002.
14. WIE, B., BAILEY, D. and HEIBERG, C. Rapid multitarget acquisition and pointing of agile spacecraft, *J Guidance, Control and Dynamics*, 2002, **25**, (1), pp 96-104.

https://doi.org/10.1017/S0001924000004589 Published online by Cambridge University Press